PPAR-γ agonist protects podocytes from injury

T Kanjanabuch[1], L-J Ma[1], J Chen[1], A Pozzi[2], Y Guan[2], P Mundel[3] and AB Fogo[1,2]

[1]*Department of Pathology, Vanderbilt University Medical Center, Nashville, Tennessee, USA;* [2]*Department of Medicine, Vanderbilt University Medical Center, Nashville, Tennessee, USA and* [3]*Division of Nephrology, Mt. Sinai School of Medicine, New York, New York, USA*

Podocyte injury and loss contribute to progressive glomerulosclerosis. Peroxisome proliferator-activated receptor-γ (PPAR-γ) is a nuclear hormone receptor, which we have found to be increased in podocytes in a variety of kidney diseases. It is not known if PPAR-γ contributes to renal injury or if it serves as a countermeasure to limit renal injury during disease progression. We tested these possibilities utilizing the puromycin aminonucleoside (PAN) model of renal injury in immortalized mouse podocytes. The cultured podocytes expressed PPAR-γ mRNA at baseline but this was decreased by PAN. Pioglitazone, a pharmacologic agonist of PPAR-γ, increased both PPAR-γ mRNA and activity in injured podocytes, as assessed by a reporter plasmid assay. Further, pioglitazone significantly decreased PAN-induced podocyte apoptosis and necrosis while restoring podocyte differentiation. The PPAR-γ agonist significantly restored expression of the cyclin-dependent kinase inhibitor p27 and the antiapoptotic molecule Bcl-xL while significantly decreasing proapoptotic caspase-3 activity. Pioglitazone tended to decrease PAN-induced transforming growth factor-β (TGF-β) mRNA expression. Our study shows that PPAR-γ is normally expressed by podocytes and its activation is protective against PAN-induced apoptosis and necrosis. We postulate that this protective effect may be mediated in part by effects on p27 and TGF-β expression.

Kidney International (2007) **71,** 1232–1239; doi:10.1038/sj.ki.5002248; published online 25 April 2007

KEYWORDS: apoptosis; cyclin-dependent kinase inhibitors; sclerosis

Correspondence: *AB Fogo, MCN C3310, Department of Pathology, Vanderbilt University Medical Center, Nashville, Tennessee 37232, USA. E-mail: agnes.fogo@vanderbilt.edu*

Received 8 May 2006; revised 16 January 2007; accepted 13 February 2007; published online 25 April 2007

Peroxisome proliferator-activated receptor-γ (PPAR-γ) is a member of the nuclear hormone receptor superfamily, and a pharmacological target for the antidiabetic thiazolidinediones.[1] PPAR-γ contains both ligand- and DNA-binding domains. PPAR-γ forms a heterodimeric complex with retinoic X receptor, translocates to the nucleus, and binds to defined PPAR response elements in the promoter regions of specific target genes. PPAR-γ agonists enhance insulin sensitivity, decrease hepatic glucose production, and decrease low-density lipoprotein levels, and thereby ameliorate both the dysmetabolic state of diabetes mellitus and its complications, including diabetic nephropathy.[1] PPAR-γ is widely expressed and has a variable role in cell-cycle regulation depending on cell type. PPAR-γ tends to inhibit cell growth and promotes differentiation, decreases inflammation, and inhibits extracellular cellular matrix accumulation.

Podocytes are terminally differentiated and highly specialized cells. Podocyte injury with subsequent depletion is a key component of progressive glomerulosclerosis, regardless of the nature of the initial insult. Mature podocytes have limited ability to proliferate following injury, linked to high expression of the cyclin-dependent kinase inhibitors (CKIs) p27 and p57, which appear to be rate-limiting for podocytes to reenter the cell cycle.[2] Another CKI, p21, appears to be necessary for development of sclerosis after 5/6 nephrectomy in mice.[3] Apoptosis may play an important role in loss of podocytes after injury. Indeed, apoptosis is increased in human focal segmental glomerulosclerosis (FSGS).[4] Thiazolidinediones may promote or protect against apoptosis, depending on cell type and nature of injury.[5–7] Numerous other factors, including transforming growth factor-β (TGF-β), may also promote podocyte apoptosis.[8] In early-stage diabetic nephropathy in humans, treatment with a PPAR-γ agonist reduced podocyturia, likely reflecting amelioration of podocyte injury, detachment, and possibly apoptosis.[9] PPAR-γ agonist also attenuated tubular epithelial cell apoptosis *in vitro*.[10] We previously showed *in vivo* that thiazolidinedione ameliorated injury both in the remnant kidney and in PAN nephropathy models, associated with increased PPAR-γ expression in podocytes.[11,12] We also observed increased podocyte PPAR-γ in human diabetic nephropathy, hypertensive nephrosclerosis, and chronic allograft nephropathy.[13–16] The association of increased PPAR-γ with sclerotic injury could suggest that PPAR-γ may induce podocyte injury and

cause glomerulosclerosis. Alternatively, increased PPAR-γ expression in podocytes after injury may be a counter-regulatory beneficial response. We therefore investigated the effects of PPAR-γ agonist on podocyte injury induced by PAN. We further examined effects of PPAR-γ activation on cell-cycle proteins, apoptosis markers, and TGF-β.

RESULTS

Podocyte morphologic changes

Treatment of cultured podocytes with 100 μg/ml PAN for 24 h resulted in process retraction, cell rounding, and detachment. Increasing dose and duration of PAN enhanced podocyte injury. Pio ameliorated, but did not prevent, PAN-induced morphologic injury (cells with differentiated foot processes; baseline or Pio alone 100%, PAN $33 \pm 6\%$ vs PAN + Pio $59 \pm 1\%$) (Figure 1). This protective effect of Pio was investigated by immunofluorescent staining with synaptopodin. At baseline (Figure 2), differentiated podocytes strongly expressed synaptopodin, a sensitive and specific marker for differentiated podocytes,[17] particularly in the cytoplasm and extending toward cell processes. In contrast, synaptopodin staining was decreased in PAN-treated podocytes, largely reflecting decreased processes. Thus, foot processes and corresponding synaptopodin protein expression were partially restored by adding Pio to injured podocytes.

Apoptosis and necrosis

To investigate podocyte apoptosis induction by PAN, we measured DNA fragmentation, a marker of the late stage of apoptosis (Figure 3). Addition of Pio appeared to decrease DNA fragmentation in response to PAN. Injury after PAN treatment was also assessed by the terminal deoxynucleotidyl transferase-mediated dUTP nick-end labeling method, with

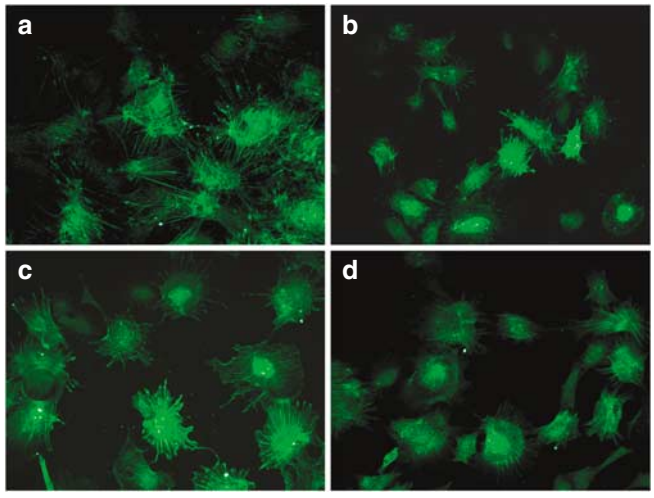

Figure 2 | Podocyte differentiation. (**a**) Podocytes treated with vehicle strongly expressed synaptopodin, particularly in the cytoplasm and extending toward cell processes. (**b**) Podocytes treated with 100 μg/ml PAN had markedly decreased foot processes with corresponding decrease in synaptopodin in most cells, with decreased staining of the retracted processes. (**c**) Podocytes treated with 0.1 μM Pio alone showed no change in extent of foot processes or synaptopodin compared with normal control. (**d**) Podocytes treated with 0.1 μM Pio + 100 μg/ml PAN showed partial maintenance of foot processes and corresponding synaptopodin staining, when compared with PAN (anti-synaptopodin immunofluorescence, original magnification $\times$ 400).

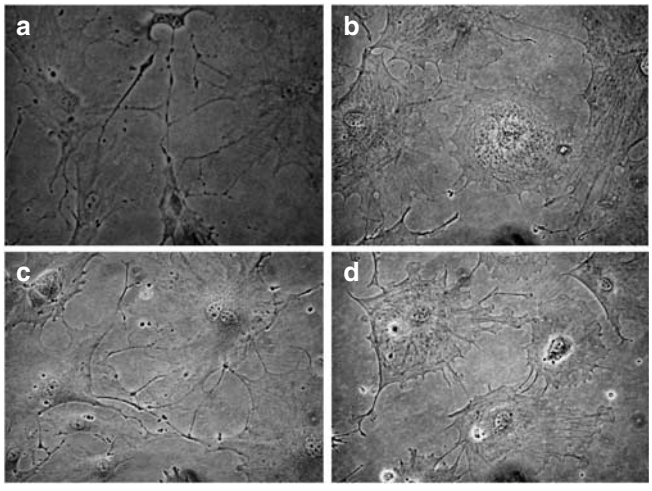

Figure 1 | Podocyte morphology. Fully differentiated cells were exposed for 24 h to vehicle (0.02% DMSO), 100 μg/ml PAN, 0.1 μM Pio, or 0.1 μM Pio + 100 μg/ml PAN as indicated. Differentiated podocytes (**a**) demonstrated fine processes with interdigitations between cells. Treatment with PAN (**b**) was associated with varying degree of process retraction, cell rounding, and detachment. Podocytes treated with 0.1 μM Pio alone (**c**) showed no change in morphology compared with normal control. However, adding Pio (**d**) partially prevented the morphologic changes induced by PAN treatment, with more complex processes and interdigitations.

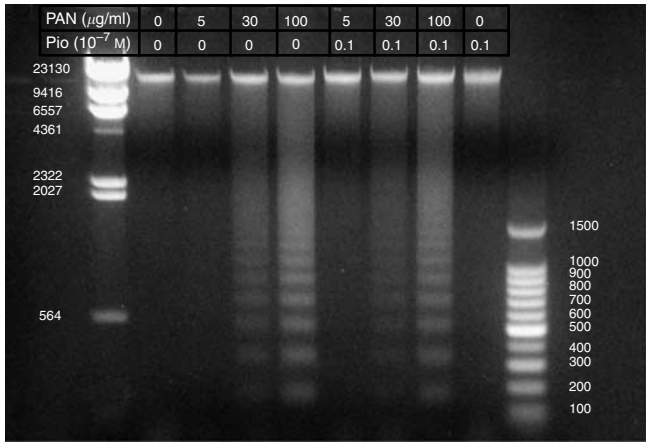

Figure 3 | DNA fragmentation in PAN-injured podocytes. Fully differentiated cells were exposed to 0.1 μM Pio and injured with variable concentrations of PAN (5, 30, and 100 μg/ml) for 24 h at 37°C. At the end of the incubation period, cells were prepared for DNA gel electrophoresis. Lanes 1 and 10 show molecular weight markers. Control (lane 2), 5 μg/ml PAN, (lane 3), and 5 μg/ml PAN + 0.1 μM Pio (lane 6) did not show any DNA fragmentation, whereas 30 and 100 μg/ml PAN (lanes 4 and 5, respectively) showed DNA ladder pattern reflecting intranucleosomal-DNA-fragment production. The laddering was fainter when PAN-injured cells also were treated with Pio (lanes 7 and 8) compared with PAN alone at same concentrations (lanes 4 and 5).

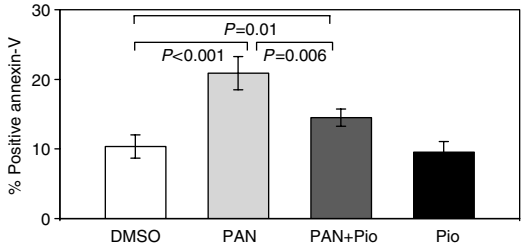

Figure 4 | Apoptosis in PAN-injured podocytes. Fully differentiated podocytes were exposed for 24 h to vehicle (0.02% DMSO), 100 μg/ml PAN, 0.1 μM Pio, or 0.1 μM Pio + 100 μg/ml PAN as indicated. Cell aliquots were stained with Annexin V-FITC and PI and analyzed by FACScan. Percentage of cells undergoing apoptosis was calculated by percentage of cells staining with Annexin V-FITC and excluding the PI dye.

no positivity in normal cells, but frequent positivity after PAN, and apparent decrease with added Pio (data not shown). We then quantitated apoptotic changes by assessing an early marker of these events, Annexin V. When cells undergo apoptosis, phosphatidylserine residues relocate to the outside of the cell membrane, which can be detected by adding the specific binding molecule, Annexin V (Figure 4). PAN induced significant apoptosis compared with untreated cells, and Pio significantly attenuated PAN-induced apoptosis (% cells apoptotic: CONT 10.4±1.7, PAN 20.1±2.4, PAN + Pio 14.5±1.2, and Pio 9.5±1.5, $P<0.01$ PAN vs dimethylsulfoxide (DMSO) control and PAN + Pio) and necrosis (% cells necrotic: CONT 0.1±0.0, PAN 4.4±1.0, PAN + Pio 1.0±0.6, and Pio 0.1±0.0). Again, Pio alone did not affect apoptosis and necrosis in normal podocytes. Lactate dehydrogenase release, a marker of cell necrosis, was increased after PAN, with no effect of Pio (DMSO 4.3±1.5 U/L, PAN 21.7±7.0, Pio 7.3±1.5, PAN + Pio 21.7±5.7, $P<0.01$ PAN vs DMSO).

Corresponding to these changes in apoptosis, there was an increase of Bax and decrease of Bcl-xL and Bcl-2 mRNA in response to PAN (Figure 5). Pio had no significant effect on Bax or Bcl-2 expression, but did increase Bcl-xL expression (Bax mRNA expression, fold changes vs CONT: CONT 1±0.11, PAN 1.56±0.28, PAN + Pio 1.59±0.43, Pio 1.48±0.50; PAN vs CONT $P<0.01$, PAN vs PAN + Pio $P=0.88$; Bcl-xL mRNA expression, fold changes vs CONT: CONT 1±0.07, PAN 0.56±0.07, PAN + Pio 0.77±0.12, Pio 1.62±0.72, $P<0.01$ PAN vs CONT and PAN + Pio; Bcl-2 mRNA expression, fold changes vs CONT: CONT 1±0.12, PAN 0.50±0.08, PAN + Pio 0.56±0.13, Pio 0.83±0.24, $P<0.01$ PAN vs CONT, $P=$ NS PAN + Pio vs PAN).

We next assessed whether these changes in mRNA of regulatory molecules of apoptosis affected protein expression of a key downstream effector of apoptosis, cleaved caspase-3. Activated caspase-3 was not detected at baseline, but was markedly increased after PAN injury, and significantly ameliorated by adding Pio (activated caspase-3/β-actin: control with DMSO 0.11±0.05, PAN 0.59±0.14, Pio 0.07±0.02, PAN + Pio 0.29±0.02, $P<0.01$ PAN vs DMSO,

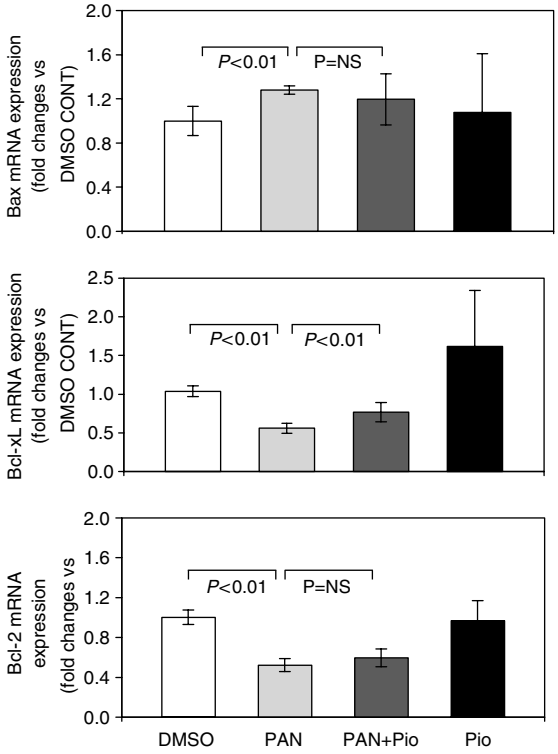

Figure 5 | Apoptotic regulatory molecule mRNA expression in podocytes. Total RNA from podocytes was harvested and Bax, Bcl-xL, and Bcl-2 mRNA expressions measured by quantitative real-time PCR. Antiapoptotic molecules Bcl-xL and Bcl-2 were downregulated after injury with PAN, whereas proapoptotic Bax was increased. Added Pio significantly increased Bcl-xL.

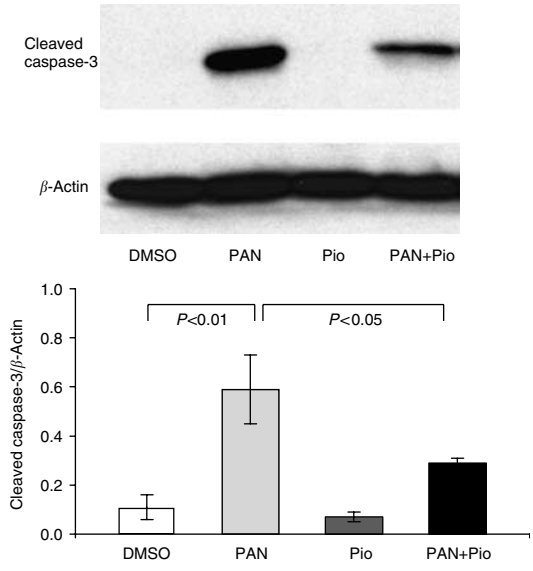

Figure 6 | Activated caspase-3 expression in podocytes. Protein from podocytes was analyzed by Western blot for total and cleaved-activated caspase-3. Activated caspase-3 was not detectable under baseline conditions, but was markedly increased after PAN injury, and ameliorated by added Pio.

and $P<0.05$ PAN + Pio vs PAN) (Figure 6). Interestingly, total caspase-3 displayed similar expression patterns after PAN with or without Pio treatment as activated caspase-3.

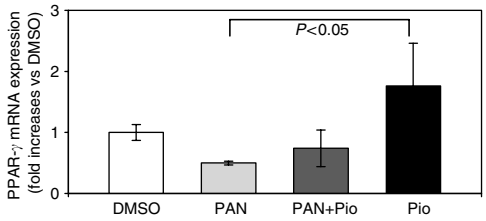

Figure 7 | PPAR-γ mRNA expression in podocytes. Total RNA from podocytes was harvested and PPAR-γ mRNA measured by quantitative real-time PCR. PPAR-γ mRNA was present in normal podocytes treated only with vehicle (DMSO), and was decreased by PAN. Pio increased PPAR-γ mRNA.

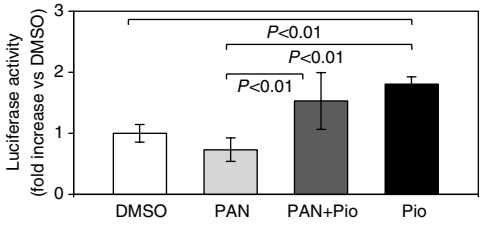

Figure 8 | Ligand-induced transcriptional activity of PPAR-γ. Transient transfection of differentiated podocytes was done using Superfect reagent with PPAR response element 3-TK-luciferase. Cells were subsequently incubated with control vehicle (DMSO) or 100 μg/ml PAN ± 0.1 μM Pio for 24 h. Luciferase activities in cell lysates were measured using a luminometer. Results are expressed as ratio to control. Pio increased PPAR-γ activity both in normal and in PAN-injured podocytes.

Effect of pioglitazone on PPAR-γ expression and activity

Quantitative real-time polymerase chain reaction (PCR) was used to assess podocyte expression of PPAR-γ (Figure 7). At baseline, podocytes expressed low level of PPAR-γ mRNA, which was decreased after exposure to PAN. Pio upregulated PPAR-γ expression both in control and PAN-injured cells, largely preventing the PAN-induced decrease in PPAR-γ (mRNA expression, fold increase vs CONT: CONT 1 ± 0.13, PAN 0.50 ± 0.03, PAN + Pio 0.74 ± 0.30, Pio 1.76 ± 0.70, $P < 0.05$ Pio vs PAN). We then examined the activity of PPAR-γ as a transcription factor using a luciferase reporter plasmid containing a PPAR-γ response element. PAN only numerically decreased PPAR-γ activity (27% decrease in luciferase vs control, pNS). In contrast, Pio resulted in increased mRNA and activated PPAR-γ (fold activation: CONT 1 ± 0.14, PAN 0.73 ± 0.19, PAN + Pio 1.53 ± 0.46, Pio 1.80 ± 0.12, $P < 0.01$ PAN + Pio and Pio vs PAN) (Figure 8).

Cellular proliferation and cell cycle and TGF-β regulation

As expected, PAN not only induced cell necrosis and apoptosis, but decreased cell proliferation, which was restored by adding Pio to injured podocytes, while adding Pio to normal podocytes had no effect (c.p.m.: CONT 28461 ± 1387, PAN 10270 ± 304, PAN + Pio 17395 ± 687, Pio 27602 ± 299, $P < 0.01$ PAN vs CONT and PAN + Pio). To investigate possible mechanisms of PPAR-γ effects on podocyte injury, apoptosis, and cell proliferation, we assessed the CKIs p27, p21, and p57 using quantitative real-time PCR. p27 was significantly downregulated after injury with PAN (46% of control, $P = 0.02$) and expression was significantly restored after combined treatment with PAN and Pio. In contrast, p21 was changed only numerically, with increase after exposure to PAN and PAN + Pio, and decrease with Pio alone. p57 mRNA was not significantly affected. PAN activated TGF-β in a dose-dependent manner (data not shown), and there was a trend for attenuation by Pio (TGF-β mRNA expression, fold increase vs CONT: CONT 1.0 ± 0.15, PAN 1.8 ± 0.49, PAN + Pio 1.0 ± 0.05, Pio 0.85 ± 0.03, $P = 0.07$ PAN + Pio vs PAN).

DISCUSSION

In this study, we show that PPAR-γ was expressed in both normal and injured podocytes. Moreover, we demonstrated that PPAR-γ is downregulated at the mRNA level following injury with PAN, and that treatment with the thiazolidinedione pioglitazone numerically increased PPAR-γ mRNA and significantly increased its activity. Pioglitazone also decreased morphological cell injury, necrosis and apoptosis, decreased activated caspase-3, and restored normal proliferation. Possible mechanisms implicated by our further studies include restored expression of a key CKI, p27, and the antiapoptotic Bcl-xL, with decreased TGF-β. These data implicate increased PPAR-γ activation as a key protective mechanism in podocyte injury.

The podocyte is a highly specialized cell with limited capacity for proliferation.[2] Mechanisms of podocyte loss and restoration of injured podocytes are therefore key for determining whether injury leads to progressive glomerulosclerosis.[18–20] In this *in vitro* system, we induced injury to podocytes with the epithelial toxin PAN.[21,22] PAN *in vitro* results in foot process retraction and variable dose-dependent cell death. *In vivo*, PAN induces injury in rats, which, depending upon dose and route of administration, results in minimal change disease or FSGS.[12,23,24] Thus, both *in vivo* and *in vitro* PAN-induced injury models are relevant for understanding mechanisms of podocyte injury. As described previously, podocytes showed altered morphology and apoptosis and necrosis when exposed to this dose (100 μM) of PAN.[21] Of note, we chose a dose with only modest lethal effects on cells, so that we might study the injury and repair response. The podocyte injury was associated with dedifferentiation of podocytes, as seen by decreases in foot process formation with corresponding decrease in immunostaining for synaptopodin, and marked decrease in proliferation. Further, the CKI p27, but not p21 or p57, was significantly downregulated in response to PAN, with increase in TGF-β mRNA. The PPAR-γ agonist pioglitazone largely restored these abnormal responses, decreasing necrosis and apoptosis, and restoring differentiation and proliferation to normal levels. That these effects of pioglitazone were mediated by specific PPAR-γ actions was verified by increased PPAR-γ transcription factor activity. Increased PPAR-γ

activity was associated with restoration of p27 and Bcl-xL mRNA levels, with decreased activated caspase-3 and attenuated TGF-β.

Podocyte growth and apoptosis are complexly regulated.[2] Bcl-2 family proteins include both proapoptotic molecules such as Bax and antiapoptotic molecules such as Bcl-xL and Bcl-2. These molecules are regulators of caspases, which serve as terminal effector molecules in many types of apoptosis. In previous studies, the group of Shankland examined cultured podocytes injured by PAN and response to dexamethasone.[25] Dexamethasone was effective in decreasing PAN-induced apoptosis and increased Bcl-xL expression along with a decrease in p53. In our studies, we observed similar alterations in Bcl-xL in response to PAN, with normalization by pioglitazone. Further, these changes were accompanied by increase in the key downstream effector of apoptosis, activated caspase-3, in response to PAN, with decrease by added pioglitazone. The potential beneficial impact of pioglitazone on podocyte injury is important, as dexamethasone has numerous side effects, which may limit its long-term utility *in vivo* as a modulator of podocyte injury and apoptosis. In our previous *in vivo* studies of PAN-induced FSGS, we found very low expression of PPAR-γ in normal kidneys, with increased PPAR-γ when injury was established.[12] This increased PPAR-γ immunostaining was particularly evident in podocytes and mesangial cells in segmentally sclerotic glomeruli. Treatment with a PPAR-γ agonist ameliorated progressive sclerosis, associated with a strong accentuation of podocyte immunohistochemical staining for PPAR-γ.[12] Our *in vitro* results support that augmented PPAR-γ protein could be a counterregulatory response to injury that induces increased PPAR-γ activation, with beneficial responses on podocyte differentiation and growth, with resulting decreased podocyte injury, and increased survival. Indeed, treatment with pioglitazone in the *in vivo* PAN model led to higher number of preserved podocytes, as judged by glomerular WT-1-positivity, compared with the untreated PAN-FSGS rats.

In additional *in vitro* studies, we examined if the restored proliferation in response to pioglitazone was linked to effects on CKIs. The podocyte highly expresses several such cyclin-dependent kinase inhibitors, including p21, p27, and p57.[2,25] However, only p27 was significantly affected in this PAN injury model. p27 expression was significantly restored by pioglitazone, associated with restoration of proliferation. Of note, these responses of the podocytes were also associated with alterations in TGF-β. TGF-β has numerous functions, including key effects on cell growth/differentiation, immune regulation, and matrix synthesis. In previous studies, conditionally immortalized podocytes had induction of G0/G1 arrest by autocrine TGF-β2 production.[8] Differentiation was also arrested. These effects were mediated through Smad-3-dependent induction of the CKI p15. TGF-β effects on podocytes were concentration-dependent, with distinctly different signaling profiles at low vs high levels. At lower levels, TGF-β induced G0/G1 arrest and differentiation of podocytes, whereas higher concentrations were associated with G2/M block and apoptosis.[8] We found in our present studies that TGF-β was increased in PAN-injured podocytes, associated with apoptosis similar to these previously reported results. Treatment with pioglitazone tended to attenuate this change, with TGF-β mRNA expression returning towards control baseline. PPAR-γ has numerous effects on a variety of genes, and is a key molecule linked to progressive sclerosis. We have previously observed in the hypertensive 5/6 nephrectomy model of FSGS that PPAR-γ agonists could decrease the upregulated TGF-β and PAI-1.[11] However, in our studies of the PAN model of sclerosis with minimal hypertension, we did not observe significant changes of TGF-β at the whole kidney level.[12] The current *in vitro* data indicate that local cell-specific podocyte alterations in TGF-β may occur in the PAN model of FSGS, and may influence podocyte apoptosis vs growth and differentiation. Further, PPAR-γ agonist may dampen such deleterious podocyte upregulation of TGF-β.

In summary, pioglitazone is effective in decreasing podocyte injury *in vitro*, with possible mechanisms including decreased apoptosis with decreased activated caspase-3, restoration of the key CKI p27 and Bcl-xL, and decreased TGF-β. Taken together with our recent *in vivo* observations, these data suggest the potential for thiazolidinediones as a therapeutic strategy in podocyte-related diseases.

MATERIALS AND METHODS

Cell culture

Studies were performed in a conditionally immortalized mouse podocyte cell line as described previously.[26] These cells carry a thermosensitive variant of the SV-40-T-antigen, which is under the control of the H-2K^b-promoter. Activity of this promoter can be enhanced by interferon-γ. Briefly, the cells were grown in type I collagen-coated flasks and propagated at 33°C in RPMI-1640 media (Gibco/Life Technologies, Grand Islands, NY, USA) containing 10% heat-inactivated fetal calf serum (Hyclone, Logan, UT, USA), 100 U/ml penicillin (Sigma, St Louis, MO, USA), 100 μg/ml (Sigma), and 10 U/ml interferon-γ (Sigma) to induce synthesis of the immortalizing T antigen. Subcultivation was done by disaggregation with 0.1% trypsin–0.01% EDTA (Sigma) in Hanks' balanced salt solution (Sigma) at 37°C after cells had reached confluence. Cells were passaged after 1:5 dilution. To initiate differentiation, cells were then plated in collagen type I-coated flasks under nonpermissive condition (37°C without interferon-γ) for at least 7 days with medium change every 3 days.

Experimental design

To determine the role of PPAR-γ in injured podocytes, fully differentiated podocytes cultured for 7–10 days at 37°C, were treated with PAN (100 μg/ml)[22,27] in the presence or absence of the PPAR-γ-specific agonist pioglitazone (0.1 μM, Pio, Takeda, Lincolnshire, IL, USA) for 24 h. This dose of Pio was based on pilot studies that showed that this dose had the maximum protective effect against PAN-induced podocyte injury. Effects of PPAR-γ on cell injury, cell cycle, differentiation, and TGF-β were then assessed in fully differentiated cells. All data are based on results from at least three independent experiments, unless otherwise indicated.

Analysis of cell morphology

Podocyte morphology was assessed qualitatively and quantitatively by examining the extent of foot process formation, determined as number of processes per cell, and percent of cells with processes longer than cell body diameter, determined from images of stained cells. For indirect immunofluorescence, cells cultured on collagen type I-coated chamber slides were fixed with 2% paraformaldehyde and 4% sucrose in phosphate-buffered saline (PBS) for 5 min at room temperature followed by permeabilization with 0.3% Triton X-100 in PBS for 5 min. After rinsing with PBS, cells were incubated with 2% fetal calf serum, 2% bovine serum albumin, and 0.2% fish gelatin in PBS for 1 h. Cells were then incubated with monoclonal mouse anti-synaptopodin antibody (Progen, Heldelberg, Germany) overnight at 4°C, followed by fluorescein isothiocyanate (FITC)-conjugated anti-mouse immunoglobulin G antibody (Vector, Burlingame, CA, USA). Cells were subsequently mounted in 15% Mowiol (Calbiochem, San Diego, CA, USA) and 50% glycerol in PBS. Normal mouse serum was used in place of specific antibody as a negative control, and showed no staining. Images of immunofluorescent cells were captured with the AxioVision software program using a Zeiss AxioCam camera attached to a Nikon Eclipse E400 microscope (Nikon Instruments, Inc., Melville, NY, USA).

Apoptosis and necrosis

DNA fragmentation was assessed by agarose gel electrophoresis performed on fully differentiated cells exposed to a dose range of PAN (5, 30, or 100 μg/ml) with or without Pio (0.1 μM) for 24 h at 37°C. At the end of the incubation period, adherent and floating cells were prepared for DNA isolation using column purification (Roche, Indianapolis, IN, USA) and DNA was subjected to electrophoresis on 1% agarose gels. The gel was examined and photographed under ultraviolet light. The terminal deoxynucleotidyl transferase-mediated dUTP nick-end labeling method was also used. The 3′-OH ends of fragmented DNA were directly labeled with tetramethylrhodamine red (TMR) red-labeled dUTP by terminal deoxynucleotidyl transferase (Roche). All nuclei were counterstained with Hoechst 33258 (Sigma) and terminal deoxynucleotidyl transferase-mediated dUTP nick-end labeling-positive and -negative nuclei were assessed under a fluorescence microscope with similar density of cells in each field viewed.

We next quantified apoptosis by assessing propidium iodide (PI) and Annexin V. Cells were seeded onto culture dishes at a density of 1000 cells/cm^3, allowed to fully differentiate and treated with PAN with or without Pio as described above. Cells were then washed twice with ice-cold PBS, trypsinized, neutralized with serum, and pelleted by centrifugation at 200*g* for 5 min. The pellets were washed once with PBS, transferred to 5 ml culture tubes and resuspended in 2 μl of PI dye and 2 μl of Annexin V-FITC (Roche). Four hundred microliters of 1 × binding buffer were added to each tube and FACscan analysis of the samples was performed within 1 h using a FACS scan equipped with Cell Quest software (BD Biosciences, San Jose, CA, USA). The following controls were used to set up compensation and quadrants: (1) unstained cells, (2) cells stained with Annexin V-FITC alone, (3) cells stained with PI alone, and (4) cells stained with both Annexin V-FITC and PI. Exclusion of PI coupled with binding of Annexin V-FITC indicates an apoptotic cell, whereas double-positive or double-negative staining indicates necrotic cells or living cells, respectively. The percentage of cells undergoing apoptosis in response to experimental maneuvers was determined by correcting for apoptosis and necrosis under baseline control conditions. Experiments were repeated three times.

Cells treated as above with DMSO, PAN, PAN with Pio, or Pio alone were assessed for lactate dehydrogenase release. Culture medium was collected and centrifuged, and the supernatant analyzed for lactate dehydrogenase activity using the lactate dehydrogenase IFCC liquid method (Roche Diagnostics).

Cell proliferation

Cell proliferation was assessed in cells treated as above by measuring the incorporation of ^{3}H-thymidine. In brief, 2500 cells were plated onto 96-well plates in complete medium, and differentiation was induced as above. Cells were then exposed to a dose range of PAN alone or with Pio as above, and 1 μCi of ^{3}H-thymidine was added, and cells incubated at 37°C for 24 h before harvest.[28] Cells were then washed three times with PBS, lysed with 100 μl 1% sodium dodecyl sulfate and the amount of ^{3}H-thymidine counted using a β-counter.

Cell transfection

To assess the extent of PPAR-γ activation, cells seeded at densities of 1000 cells/cm^3 in 6-well plates and then fully differentiated, were transiently transfected with the PPAR response element 3-TK-luciferase vector, a reporter construct with a PPAR-γ response element derived from the PPAR-γ target gene acyl-CoA oxidase.[29] PPAR-γ-mediated promoter activation was then assessed using Superfect reaction (QIAGEN, Valencia, CA, USA) according to the developer's instruction. The cells were simultaneously cotransfected with the phRL-TK vector, a *Renilla* luciferase–thymidine kinase plasmid (Promega, Madison, WI, USA) as control to assess transfection efficiency. Cells were then treated as above for 24 h with a dose range of PAN with or without Pio. Firefly and *Renilla* luciferase activities in cell lysates were then measured (Promega assay kit). Luciferase activity was measured using a TD-20/20 luminometer. To correct for differences in transfection efficiency, firefly luciferase units were normalized for *Renilla* luciferase activity

Table 1 | Primer and probe sequences

Name	DNA sequence from 5′–3′		
	Forward primer	Probe	Reverse primer
PPAR-γ	CTGTTATGGGTGAAACTCTGGGAG	6FAM-TCCTGTTGACCCAGAGCATGGTGC-TAMRA	ATAGGCAGTGCATCAGCGAA
TGF-β	GCAACATGTGGAACTCTACCAGAA	6FAM-ACCTTGGTAACCGGCTGCTGACCC-TAMRA	GACGTCAAAAGACAGCCACTCA
P21	CCGTTGTCTCTTCGGTCCC	6FAM-TGGACAGTGAGCAGTTGCGCCG-TAMRA	CATGAGCGCATCGCAATC
P27	TTTTCCGGAGAGAGGCGAG	6FAM-CGGTGGTCCACACCCGCCC-TAMRA	CTCACGTTTGACATCTTCCTCCT
P57	CAGCGGACGATGGAAGAACT	6FAM-TGGGCTTCGGCTGGGACCTTTC-TAMRA	CTCCGGTTCCTGCTACATGAA
Bcl-2	CTGAGTACCTGAACCGGCATC	6FAM-CCCCAGCATGCGACCTCTGTTTG-TAMRA	GAGCAGCGTCTTCAGAGACAG
Bcl-xL	TGACCACCTAGAGCCTTGGAT	6FAM-CGGGAACAATGCAGCAGCCGAG-TAMRA	CAGGAACCAGCGGTTGAAA
Bax	GTTTCATCCAGGATCGAGCAG	6FAM-AGCTGAGCGAGTGTCTCCGGCG-TAMRA	AGCTGAGCGAGTGTCTCCGGCG

in the same lysate. The normalized readings were subtracted with empty vector readings.

Real-time quantitative reverse transcriptase-polymerase chain reaction

Total RNA was extracted from cells as previously described[11]. Quantitation of gene expression was performed by real-time quantitative reverse transcriptase-polymerase chain reaction using the ABI PRISM® 7700 Sequence Detection System (PE Applied Biosystems, Foster City, CA, USA). A 25-μl PCR reaction mixture containing 1 μl of cDNA, 1 TaqMan PCR Master Mix (PE Applied Biosystems), 810 ng of gene-specific forward and reverse primers and 6.25 μM of the corresponding real-time PCR probe at final concentrations was used. Primers and probes designed to target mouse PPARγ, p21, p27, p57, Bax, Bcl-2, Bcl-xL, and TGFβ are listed in Table 1. The reaction conditions were designed as follows: initial denaturation at 95°C for 10 min followed by 40 two-step cycles with 30 s at 95°C for denaturing and 1 min at 60°C for annealing and extension. The threshold cycle, that is the cycle number at which the amount of amplified gene of interest reached a fixed threshold, was subsequently determined. Relative quantification of each target mRNA level was normalized to 18S rRNA and calculated by the comparative threshold cycle method described elsewhere.[30]

Western blot of activated caspase-3

Cells treated as above with DMSO, PAN with or without Pio, or Pio alone (including floating cells) were harvested and lysed in modified radioimmunoprecipitation assay lysis buffer with protease and phosphatase inhibitors as described previously.[31] Protein samples (30 μg) were separated on 12% sodium dodecyl sulfate-polyacrylamide gel electrophoresis, transferred to a polyvinylidene difluoride membrane, blocked in 5% non-fat dried milk in Tris-buffered saline Tween (TBS and 0.01% Tween 20), and incubated overnight (4°C) with the following primary antibodies: anti-cleaved caspase-3 antibody (Asp175, Cat#9661, Cell Signaling Technology, Danvers, MA, USA) or anti-caspase-3 antibody 1:500 (Cat no. 9662, Cell Signaling). After washing, secondary antibody was added and incubated 1 h at room temperature and protein bands were visualized by ECL Plus (Amersham, Arlington Heights, IL, USA). The membranes were then stripped and re-probed with mouse anti-β-actin antibody (Sigma). Densitometric quantitation was performed using NIH image (version 1.63). Protein expression was quantified as the ratio of specific band to β-actin. Experiments were performed and repeated independently twice.

Statistical analysis

Data are presented as means $\pm$ s.e.m., unless otherwise noted. *P*-values were calculated by analysis of variance followed by unpaired *t*-test with correction for multiple comparisons as appropriate. A $P < 0.05$ was considered to be significant.

ACKNOWLEDGMENTS

We thank Ellen Donnert and Suli Mao for expert technical assistance. This study was supported in part by a grant from Takeda Pharmaceuticals North America Inc. and a grant from the NIH DK56942.

REFERENCES

1. Guan Y, Breyer MD. Peroxisome proliferator-activated receptors (PPARs): novel therapeutic targets in renal disease. *Kidney Int* 2001; **60**: 14–30.
2. Marshall CB, Shankland SJ. Cell cycle and glomerular disease: a minireview. *Nephron Exp Nephrol* 2006; **102**: e39–e48.
3. Megyesi J, Price PM, Tamayo E *et al.* The lack of a functional p21(WAF1/CIP1) gene ameliorates progression to chronic renal failure. *Proc Natl Acad Sci USA* 1999; **96**: 10830–10835.
4. Szabolcs MJ, Ward L, Buttyan R *et al.* Apoptosis elucidated by labeling for DNA fragmentation in human renal biopsies (abstract). *Lab Invest* 1994; **70**: 160A.
5. Chinetti G, Griglio S, Antonucci M *et al.* Activation of proliferator-activated receptors alpha and gamma induces apoptosis of human monocyte-derived macrophages. *J Biol Chem* 1998; **273**: 25573–25580.
6. Rovin BH, Wilmer WA, Lu L *et al.* 15-Deoxy-delta12.14-prostaglandin J2 regulates mesangial cell proliferation and death. *Kidney Int* 2002; **61**: 1293–1302.
7. Gouni-Berthold I, Berthold HK, Weber AA *et al.* Troglitazone and rosiglitazone induce apoptosis of vascular smooth muscle cells through an extracellular signal-regulated kinase-independent pathway. *Naunyn-Schmiedebergs Arch Pharmacol* 2001; **363**: 215–221.
8. Wu DT, Bitzer M, Ju W *et al.* TGF-β concentration specifies differential signaling profiles of growth arrest/differentiation and apoptosis in podocytes. *J Am Soc Nephrol* 2005; **16**: 3211–3221.
9. Nakamura T, Ushiyama C, Osada S *et al.* Pioglitazone reduces urinary podocyte excretion in type 2 diabetes patients with microalbuminuria. *Metab: Clin Exp* 2001; **50**: 1193–1196.
10. Haraguchi K, Shimura H, Onaya T. Activation of peroxisome proliferator-activated receptor-gamma inhibits apoptosis induced by serum deprivation in LLC-PK1 cells. *Exp Nephrol* 2002; **10**: 393–401.
11. Ma LJ, Marcantoni C, Linton MF *et al.* Peroxisome proliferator-activated receptor-gamma agonist troglitazone protects against nondiabetic glomerulosclerosis in rats. *Kidney Int* 2001; **59**: 1899–1910.
12. Yang HC, Ma LJ, Ma J *et al.* Peroxisome proliferator-activated receptor-gamma agonist is protective in podocyte injury-associated sclerosis. *Kidney Int* 2006; **69**: 1756–1764.
13. Marcantoni C, Ma LJ, Federspiel C *et al.* Hypertensive nephrosclerosis in African Americans versus Caucasians. *Kidney Int* 2002; **62**: 172–180.
14. Paueksakon P, Revelo MP, Ma LJ *et al.* Microangiopathic injury and augmented PAI-1 in human diabetic nephropathy. *Kidney Int* 2002; **61**: 2142–2148.
15. Marcantoni C, Ma LJ, Donnert E *et al.* Plasminogen activator inhibitor-1 (PAI-1) and peroxisome proliferator-activated receptor-γ (PPAR-γ) in hypertensive nephrosclerosis (abstract). *J Am Soc Nephrol* 2000; **11**: 351A.
16. Revelo MP, Federspiel C, Helderman H *et al.* Chronic allograft nephropathy: expression and localization of PAI-1 and PPAR-gamma. *Nephrol Dial Transplant* 2005; **20**: 2812–2819.
17. Mundel P, Heid HW, Mundel TM *et al.* Synaptopodin: an actin-associated protein in telencephalic dendrites and renal podocytes. *J Cell Biol* 1997; **139**: 193–204.
18. Kim YH, Goyal M, Kurnit D *et al.* Podocyte depletion and glomerulosclerosis have a direct relationship in the PAN-treated rat. *Kidney Int* 2001; **60**: 957–968.
19. Kretzler M. Role of podocytes in focal sclerosis: defining the point of no return. *J Am Soc Nephrol* 2005; **16**: 2830–2832.
20. Matsusaka T, Xin J, Niwa S *et al.* Genetic engineering of glomerular sclerosis in the mouse via control of onset and severity of podocyte-specific injury. *J Am Soc Nephrol* 2005; **16**: 1013–1023.
21. Bertram JF, Messina A, Ryan GB. *In vitro* effects of puromycin aminonucleoside on the ultrastructure of rat glomerular podocytes. *Cell Tissue Res* 1990; **260**: 555–563.
22. Fishman JA, Karnovsky MJ. Effects of the aminonucleoside of puromycin on glomerular epithelial cells *in vitro*. *Am J Pathol* 1985; **118**: 398–407.
23. Caulfield JP, Reid JJ, Farquhar MG. Alterations of the glomerular epithelium in acute aminonucleoside nephrosis. Evidence for formation of occluding junctions and epithelial cell detachment. *Lab Invest* 1976; **34**: 43–59.
24. Anderson S, Diamond J, Karnovsky M *et al.* Mechanisms underlying transition from acute glomerular injury to late glomerular sclerosis in a rat model of nephrotic syndrome. *J Clin Invest* 1988; **82**: 1757–1768.
25. Wada T, Pippin JW, Marshall CB *et al.* Dexamethasone prevents podocyte apoptosis induced by puromycin aminonucleoside: role of p53 and Bcl-2-related family proteins. *J Am Soc Nephrol* 2005; **16**: 2615–2625.
26. Mundel P, Reiser J, Zuniga Mejia Borja A *et al.* Rearrangements of the cytoskeleton and cell contacts induce process formation during differentiation of conditionally immortalized mouse podocyte cell lines. *Exp Cell Res* 1997; **236**: 248–258.
27. Sanwal V, Pandya M, Bhaskaran M *et al.* Puromycin aminonucleoside induces glomerular epithelial cell apoptosis. *Exp Mol Pathol* 2001; **70**: 54–64.

28. Pozzi A, Moberg PE, Miles LA *et al.* Elevated matrix metalloprotease and angiostatin levels in integrin alpha 1 knockout mice cause reduced tumor vascularization. *Proc Natl Acad Sci USA* 2000; **97**: 2202–2207.
29. Zheng F, Fornoni A, Elliot SJ *et al.* Upregulation of type I collagen by TGF-beta in mesangial cells is blocked by PPARgamma activation. *Am J Physiol Renal Physiol* 2002; **282**: F639–F648.
30. Garcia-Villalba P, Denkers ND, Wittwer CT *et al.* Real-time PCR quantification of AT1 and AT2 angiotensin receptor mRNA expression in the developing rat kidney. *Nephron Exp Nephrol* 2003; **94**: e154–e159.
31. Ma LJ, Yang H, Gaspert A *et al.* Transforming growth factor-beta-dependent and -independent pathways of induction of tubulointerstitial fibrosis in beta6(−/−) mice. *Am J Pathol* 2003; **163**: 1261–1273.